PERMAFROST AND PERIGLACIAL PROCESSES
Permafrost and Periglac. Process., **22**: 199–213 (2011)
Published online 10 June 2011 in Wiley Online Library
(wileyonlinelibrary.com) DOI: 10.1002/ppp.724

Vegetation Canopy and Radiation Controls on Permafrost Plateau Evolution within the Discontinuous Permafrost Zone, Northwest Territories, Canada

L. Chasmer,[1]* *W. Quinton,*[1] *C. Hopkinson,*[2] *R. Petrone*[1] *and P. Whittington*[3]

[1] Cold Regions Research Centre, Wilfrid Laurier University, Waterloo, ON, Canada
[2] Applied Geomatics Research Group, NSCC, Lawrencetown, NS, Canada
[3] Department of Geography, University of Waterloo, Waterloo, ON, Canada

ABSTRACT

This study examines the links between the spatial distribution of three-dimensional vegetation structural characteristics and historical permafrost plateau area changes using airborne light detection and ranging and aerial photography. The results show that vegetation is prone to reduced canopy fractional cover (by up to 50%) and reduced canopy heights (by 16–30%) at the edges of plateaus. Reduced biomass may cause a positive feedback, whereby diminished within- and below-canopy shadowing (by 1 h of shadow time per day) results in increased radiation incident on the ground surface (16% greater at open- vs closed-canopy plateau sites) and increased longwave radiation losses (74% greater at open- vs closed-canopy plateau sites). Increased incident shortwave radiation may result in augmented thawing of permafrost and increased meltwater runoff, which further inhibits vegetation and permafrost persistence. Edge influences on ground thaw cause vegetation to die over several years (confirmed using historical aerial photography), thereby exacerbating thaw and plateau area reduction (plateau area reduction = ~27% over 60 years). Permafrost degradation is also evidenced by the increasingly fragmented characteristics of the landscape. Copyright © 2011 John Wiley & Sons, Ltd.

KEY WORDS: vegetation; discontinuous permafrost; peat plateaus; remote sensing; climate change

INTRODUCTION

The southern boundary of the discontinuous permafrost zone of northwestern Canada is characterised by tree-covered permafrost plateaus that rise 0.5 to 2 m above the surrounding bogs and channel fens (Tarnocai *et al.*, 2004). Previous research within this region indicates that: (1) historically, the size and shape of permafrost plateaus have been highly dynamic and are currently undergoing areal reduction (e.g. Shur and Jorgenson, 2007); and (2) senescence and death of vegetation determined using aerial photography from 1947 to 2000 occur mainly as a result of permafrost thaw and ground saturation at the edges of plateaus (Robinson and Moore, 2000; Robinson, 2002; Quinton *et al.*, 2010). The conversion from plateaus into permafrost-free wetlands (bogs and channel fens) affects the hydrological behaviour of drainage basins. Permafrost plateaus generate a large amount of runoff owing to the relatively large hydraulic gradient between plateaus and adjacent bogs and fens. Water entering channel fens moves downstream towards the basin outlet via lateral flow along broad, hydraulically rough channels (Quinton *et al.*, 2009). The largest proportion of water enters isolated bogs and is removed through evaporation or groundwater recharge (Quinton *et al.*, 2009). Therefore, each land cover type has contrasting hydrological functions that are affected by area changes over time. Consequently, the current state of northern water resources could change as a result of increasing stresses on permafrost via climate change and anthropogenic disturbance.

The maximum annual depth of ground thaw is limited by the cumulative annual energy flux into the ground (Rouse, 1984). A sustained increase of this flux could result in thaw of the underlying permafrost (Comiso and Parkinson, 2004). Numerous studies have related canopy structural characteristics to vegetation succession and the state of the underlying permafrost. For example, Shur and Jorgenson (2007) demonstrated that late-succession black spruce canopies promote permafrost development because they increase evapotranspiration, thereby reducing surface soil

* Correspondence to: L. Chasmer, Cold Regions Research Centre, Department of Geography, Wilfrid Laurier University, Waterloo, ON, Canada N2L 3C5. E-mail: lechasme@yahoo.ca

Received 20 August 2010
Revised 14 February 2011
Accepted 14 February 2011

moisture. Black spruce canopies efficiently intercept snow when compared to patchy shrub vegetation and open areas of mosses. This causes a reduction in ground surface snow cover and reduced insulation (Shur and Jorgenson, 2007). As vegetation regresses from late successional stages (treed canopies) to low shrubs (with treeless canopies), permafrost is preserved owing to thermal insulation of the accumulated peat (Shur and Jorgenson, 2007). Tarnocai *et al.* (2004) demonstrated that local variability of soil type and texture, soil drainage, vegetation cover and snow interception by canopies resulted in large local variability of thaw depths in a wide range of organic-covered permafrost terrains. Pomeroy *et al.* (2008) showed that the three-dimensional distribution of canopy elements (e.g. foliage area, canopy gaps, stems and branches) varied patterns of direct and diffuse radiation incident on the ground surface. Wright (2009) suggested that sunflecks and shadowing by trees added to the spatial and temporal variation of shortwave radiation (K↓) reaching the ground surface below the canopy. She also reported that the net all-wave radiation (Q*) was on average ~17 per cent less below the tree canopy of permafrost plateaus than on the adjacent treeless wetland surfaces. The canopy-controlled pattern of incident solar radiation affects the spatial distribution of snow ablation within open or closed and varying tree canopies (e.g. Pomeroy *et al.*, 2008). During ground thawing, the canopy also influences the spatial pattern of soil thaw (Anisimov *et al.*, 2002; Wright *et al.*, 2009), and therefore the pattern of subsurface drainage directions as water flows toward areas of deeper thaw (Quinton *et al.*, 2009).

Ground-based field observations are essential for gaining insight into point or plot-scale thaw processes, but they shed little light on thaw processes and patterns at the larger scale of individual or groups of plateaus. Furthermore, field measurements are limited by the relatively long time scale of some of the governing processes. For large area studies of landscape transition, the spatial distribution of vegetation canopy structural characteristics within the discontinuous permafrost zone may be used as a surrogate for permafrost area change or reduction, especially along plateau edges. This study uses tower-based radiation measurements and remote sensing data to: (1) quantify the spatial variability of vegetation structural characteristics along plateau edges where the greatest historical changes in permafrost area have occurred; (2) determine if significant differences in canopy structure exist between plateau edges and the topographically highest parts of plateaus; and (3) determine if plateau fragmentation occurs, in part, as a result of reduced cumulative tree shadow periods and measured solar insolation.

STUDY AREA

Scotty Creek (61.44°N, −121.25°W), located approximately 50 km south of Fort Simpson, Northwest Territories, Canada, drains a 152-km^2 wetland-dominated catchment with discontinuous permafrost (Figure 1). The region is characterised by short summers and long, cold winters, typical of a dry continental climate. Average annual air temperature (1971–2000) is −3.2°C and annual precipitation is approximately 370 mm, of which 46 per cent fall as snow (Quinton *et al.*, 2009). Annual average air temperatures measured by Environment Canada at Fort Simpson (located within 15 km of Scotty Creek) have increased by approximately 1.6°C since 1970.

The watershed is typical of a continental high boreal wetland region in the discontinuous permafrost zone (National Wetlands Working Group, 1997). Fens and bogs within the Scotty Creek basin occupy topographic lows and support a water table at or near the ground surface throughout the year as they receive drainage water from permafrost plateaus (Quinton *et al.*, 2003). Fens are broad, hydrologically rough channels that support a mat of floating or partly submerged *Sphagnum riparium* (Angstr.) peat, sedges, herbs and short shrubs (Quinton *et al.*, 2003). Bogs contain little woody vegetation, except along their margins, and are characterised by yellow sphagnum (Quinton *et al.*, 2003). Permafrost plateaus, on the other hand, rise 0.5 to 2 m above the surrounding fens and bogs and support trees (e.g. *Picea mariana* Mill.), shrubs, lichens and mosses (Quinton *et al.*, 2003) (Table 1). Approximately 43 per cent of the Scotty Creek watershed consists of permafrost plateaus, 24 per cent connected bogs, 21 per cent channel fens, 9 per cent lakes and 4 per cent isolated bogs (Quinton *et al.*, 2003).

A permafrost plateau forms when a sphagnum mound in a bog grows to a sufficient height above the water table to enable tree growth (Robinson and Moore, 2000; Quinton *et al.*, 2003) and to develop sufficiently cold ground temperatures (owing to greater exposure to the atmosphere and reduced thermal insulation by snow). This promotes an interannual ice lens that grows and evolves into permafrost (Wright *et al.*, 2009). The discontinuous permafrost table at Scotty Creek exists at a depth of about 1 to 2 m below the ground surface with the base of the permafrost at up to 10 m depth (Quinton *et al.*, 2009). Vegetation structure, topography and spectral characteristics of fens, bogs and permafrost plateaus are unique and allow for relatively unambiguous classification of land cover features using spectral remote sensing techniques (Quinton *et al.*, 2003).

Elevations in the study area (Figure 1) range from ~267 m in the northern part of the basin to 272 m in the south. Slopes within the Scotty Creek sub-area vary from approximately 0° to 3° within bogs and channel fens, and typically range from <3° to 20° at the boundaries between fen/bog and permafrost plateaus. However, at the resolution of the digital elevation model (DEM) (1 m), the slopes of small (within cell) hummocks and hollows are averaged.

Elevation variability and roughness due to hummocks, hollows and fallen/decaying vegetation within permafrost plateaus are greater than within fens and bogs, resulting in within-plateau slope variability (roughness) ranging from 3° to 6°. Light Detection And Ranging (LiDAR) return horizontal and vertical accuracies at Scotty Creek are beyond the scope of this study. Other studies (e.g. Hopkinson *et al.*, 2005) have examined horizontal accuracies of ground

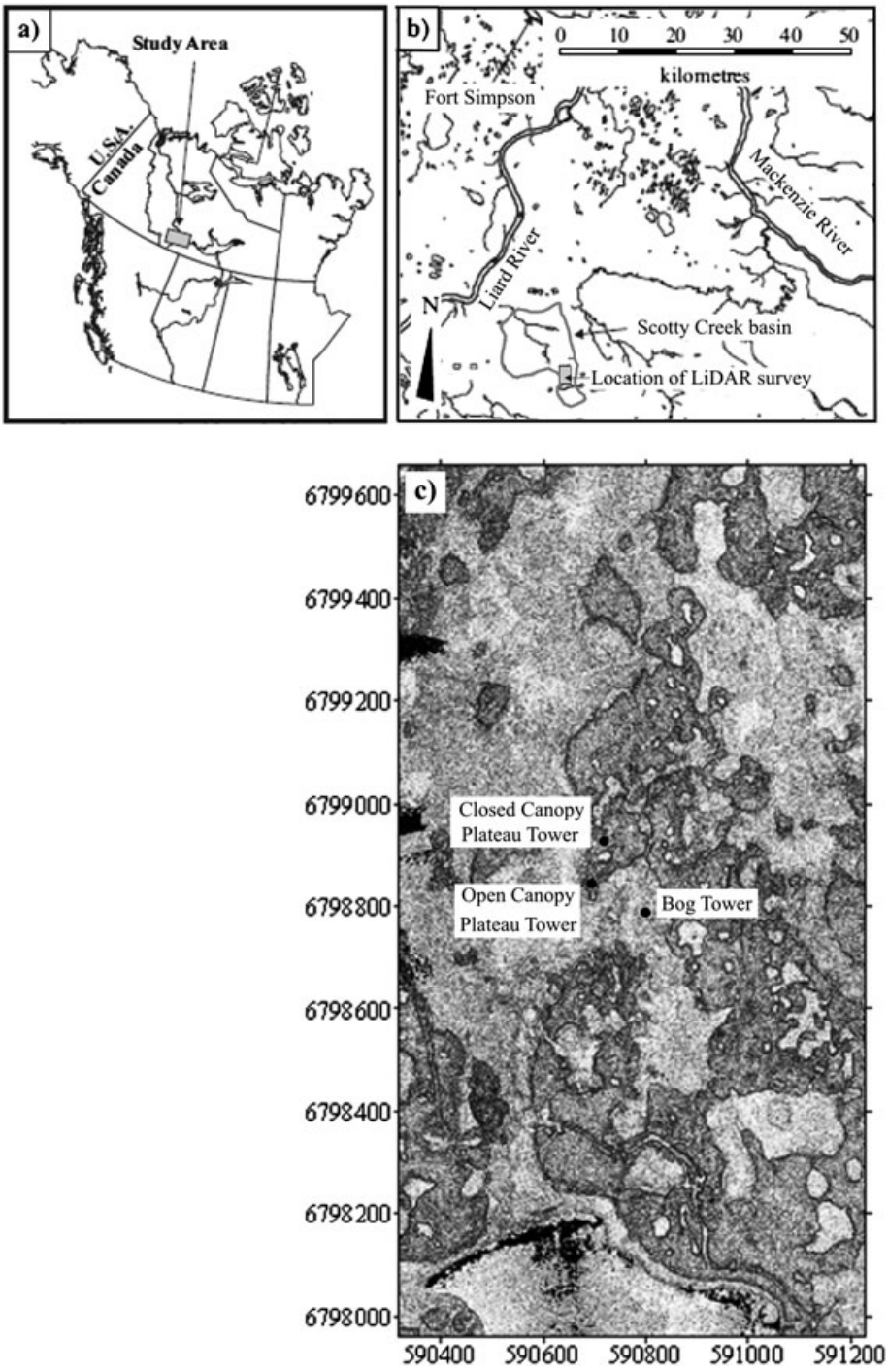

Figure 1 (a) Location of the Scotty Creek study area in the Northwest Territories, Canada; (b) map of rivers and lakes near Fort Simpson showing locations of the Scotty Creek watershed between the Mackenzie and Liard Rivers and the light detection and ranging (LiDAR) survey; (c) laser return intensity (energy) map (WGS-84 UTM zone 10) illustrating differences between forested plateaus (reduced intensity due to multiple returns) and brighter bogs and fens (single returns). Also illustrated are the locations of the closed-canopy and open-canopy plateaus and bog meteorological stations.

surface elevation and vegetation canopy heights within northern boreal peatland/wetland environments. Hopkinson *et al.* (2005) found that saturated ground conditions and standing water likely reduced the accuracy of ground elevations within areas containing aquatic wetland vegetation. Canopy heights were underestimated by 3 per cent within mature black spruce and aspen forest stands, and by up to 64 per cent within areas containing aquatic vegetation.

Table 1 Vegetation species types, average structural characteristics and average per cent cover observed within 1-m^2 mensuration plots on permafrost plateaus (n = 23) and bogs (n = 10, including bare soil).

Land cover type	Dominant species name		Vegetation type	Range of per cent cover per type (average of all plots)
	Common	Latin		
Permafrost plateau	Black spruce	*Picea mariana*	Tree	Trees: 0 to 45 (13)
	Small bog cranberry	*Oxycoccus microcarpus*	Shrub	Shrubs: 15 to 100 (56)
	Common Labrador tea	*Ledum groenlandicum*	Shrub	Lichens: 1 to 100 (65)
	Grey reindeer lichen	*Cladina rangiferina*	Lichen	Moss: 0 to 99 (26)
	Green reindeer lichen	*Cladina mitis*	Lichen	
	False pixie-cup lichen	*Cladonia chlorophaea*	Lichen	
	Rusty peat moss	*Meesia uliginosa*	Moss	
	Tall clustered thread moss	*Bryum pseudotriquetrum*	Moss	
	Yellow star moss	*Campylium stellatum*	Moss	
	Acute-leaved peat moss	*Sphagnum capillifolium*	Moss	
Bog	Black spruce	*Picea mariana*	Tree	Trees: 0 to 25 (8)
	Leatherleaf	*Chamaedaphne calyculata*	Shrub	Shrubs: 17 to 51 (30)
	Small bog cranberry	*Oxycoccus microcarpus*	Shrub	Lichens: 11 to 89 (43)
	Lingonberry	*Vacinium vitis-idaea*	Shrub	Moss: 0 to 89 (40)
	Dwarf bog rosemary	*Andromeda polifolia*	Shrub	
	Common Labrador tea	*Ledum groenlandicum*	Shrub	
	Grey reindeer lichen	*Cladina rangiferina*	Lichen	
	Green reindeer lichen	*Cladina mitis*	Lichen	
	Flattened snow lichen	*Flavocetraria nivalis*	Lichen	
	False pixie-cup lichen	*Cladonia chlorophaea*	Lichen	
	Rusty peat moss	*Meesia uliginosa*	Moss	
	Tall clustered thread moss	*Bryum pseudotriquetrum*	Moss	

Note: Mensuration plots were not examined within fens. Species that occur in one land cover type but not the other are listed in **bold**. Total and average per cent cover do not equal 100 per cent because a combination of plots were examined, all with varying per cent cover per plot.

DATA COLLECTION AND PROCESSING

LiDAR Data

LiDAR data were collected by the Applied Geomatics Research Group (AGRG, Nova Scotia, Canada) on 6 August 2008 using an Airborne Laser Terrain Mapper (ALTM) 3100 scanning, discrete four-pulse return system (Optech Inc., Toronto, Canada). The LiDAR was flown at a height of 1300 m above ground level (a.g.l.) and a scan angle of ± 18° with 50 per cent overlap of scan lines, ensuring that vegetation visible to the receiving optics was viewed from two directions, thereby limiting laser return 'shadowing' within the canopy. A pulse repetition frequency of 71 kHz was used, resulting in an approximate return spacing of 0.82 m per scan line (~ 0.40 m at 50% overlap of scan lines, or up to four returns per m^2).

All data collected by the ALTM 3100 (laser pulse ranges, aircraft movement and GPS trajectories) were combined within POSPAC (Applanix Inc., Toronto, Canada) and DashMap (Optech Inc.) proprietary software packages at the AGRG to create a matrix of x, y and z coordinates and intensities of laser return at the location where the laser pulse reflects from an object near or at the ground surface. Following the initial processing of laser ranges, aircraft movement and GPS trajectories, laser return files were imported into TerraScan software (Terrasolid, Jyväskylä, Finland) for checking/adjustment of horizontal and vertical flight-line accuracy, classification of ground and non-ground returns, and subsetting of measurement transects. The 2008 Scotty Creek LiDAR dataset was also filtered for all outlying laser returns (which were removed) and then classified into laser returns that reflected from the ground surface (P_{ground}) and those that reflected from >0.7 m above the ground surface (P_{canopy}) (to include low branches). The combined returns (or 'all returns') were saved into a separate 'all' file (P_{all}).

Spectral Remote Sensing Data

High-resolution aerial photography (1947, 1970 and 1977, pixel resolution ranging between 0.53 m and 1.1 m) and digital imagery (acquired in September 2000, IKONOS, pixel resolution = 4 m; and 2008, pixel resolution = 0.18 m, resampled to 1 m) were used to quantify vegetation change (as a proxy for permafrost plateau area change). Methods and error analysis are described in Chasmer *et al.* (2011). Multispectral (blue, green, red (visible) and near-infrared (NIR) bands) IKONOS satellite imagery was subset to match the area of LiDAR data coverage (Quinton *et al.*, 2003). Panchromatic NIR digital aerial photography was acquired coincident to and integrated with the ALTM 3100 between

1700 h and 1800 h (local time). Digital images were then mosaiced, clipped, colour-balanced and orthorectified within Terraphoto software (Terrasolid, Jyväskylä, Finland). For comparison purposes, the NIR channel of the IKONOS imagery was compared with the 2008 (NIR) aerial imagery so that spectral differences as a result of vegetation and ground surface characteristics between land cover types (plateau, bog and fen) would be maintained.

Radiation Measurements

Three sites containing meteorological and hydrological instrumentation were established at Scotty Creek between 2001 (open-canopy permafrost plateau, PPopen) and 2007 (closed-canopy permafrost plateau, PPclosed and flat bog, Bog) (Hayashi *et al.*, 2007; Wright *et al.*, 2009). Net radiation (Q*) and incident and reflected shortwave (K↓, K↑) and longwave (L↓, L↑) radiation were measured every minute and averaged over 30-min intervals from 1 January to 31 December 2007 (PPopen and Bog) and from 8 April to 17 August 2007 (PPclosed) using a four-component net radiometer (Wm^{-2}) (CNR1, Kipp and Zonen Inc., Delft, The Netherlands). Radiation sensors were located at approximate heights of 1.5 m a.g.l (Bog), 1.7 m a.g.l. (PPopen) and 1.3 m a.g.l. (PPclosed) in areas of slightly varying topography (all sensors located at approximately 1.5 m a.g.l. when average topography surrounding the sensor was considered). Sensors were used to quantify daily average energy balance differences between sites and canopy characteristics.

ANALYTICAL METHODS

Remote Sensing Change Detection

To determine differences in area extent of permafrost plateaus from historical imagery, plateaus were manually delineated based on vegetation canopy spectral characteristics, assuming a high spatial correlation between forest cover and plateau area (Chasmer *et al.*, 2011). Manual delineation was performed using spectral thresholding of bogs/fens and forested plateaus. This method divides areas of spectrally bright (high and intermediate albedo) bogs and fens and spectrally dark (low albedo) forest cover. Spectral classification procedures were also applied using up to 40 training areas per land cover type. This resulted in significant confusion (> 30%) between water-saturated (low albedo) and dry (high albedo) areas in bogs and fens and other land cover types within both IKONOS and digital imagery. Therefore, it was decided that manual delineation would likely be more accurate. Forested permafrost plateau delineation accuracy and validation using GPS transects and an airborne LiDAR DEM is discussed in Chasmer *et al.* (2011). Changes in permafrost plateau area coverage between 2000 and 2008 were estimated by subtracting the manually delineated 2008 from 2000 permafrost plateaus.

LiDAR-derived Metrics

In this study, LiDAR data are used to measure the spatial variability in canopy structure on permafrost plateaus. After classification of LiDAR returns within TerraScan, ground returns (P_{ground}) were used to create a DEM with a 1-m grid cell size from which P_{all} and P_{canopy} could be normalised relative to the ground surface (used to estimate vegetation height). DEMs were created in Golden Software Surfer (Golden Software Inc., Golden, CO, USA) using an inverse distance-weighting procedure (IDW) (O'Sullivan and Unwin, 2003) with an x, y search radius of 2 m and a power of 1, such that return integrity (z-value) was retained. Canopy height models (CHMs) were then created based on the normalised maximum z-height (m) from P_{canopy}, also using an IDW procedure at 1-m resolution, a search radius of 2 m and a power of 2. Fractional cover estimates from LiDAR (*f*cover) (where 1 = full canopy cover and 0 = no canopy cover) were determined from P_{all} and P_{canopy} returns based on the ratio between the cumulative number of canopy returns to all returns within 1 m × 1 m × height columns:

$$f\text{cover} = \left(\frac{\sum P_{canopy}}{\sum P_{all}}\right). \quad (1)$$

The 'return ratio' method used in Equation 1 has been examined in various forms within numerous studies (e.g. Todd *et al.*, 2003; Morsdorf *et al.*, 2006; Solberg *et al.*, 2006; Chasmer *et al.*, 2008; Hopkinson and Chasmer, 2009) and is regarded as an effective relative indicator of variations in foliage density, despite some underestimation of *f*cover within short canopies similar to those found at Scotty Creek (e.g. Chasmer *et al.*, 2008).

Classification of Vegetation Height Characteristics within Low-lying and Plateau Areas

Classification of permafrost plateaus and low-lying areas within the 2008 Scotty Creek LiDAR dataset was performed using Surfer and ArcGIS (ESRI Inc., Redlands, CA, USA). Detrending of the north-to-south elevation gradient throughout Scotty Creek was required to differentiate between relatively high areas (permafrost plateaus) and lower areas (fens and bogs). The detrending procedure makes the elevation gradient equal to zero so that permafrost plateaus within higher vs lower elevations can be classified relative to the surrounding lower elevation terrain. To detrend the elevation gradient, low-pass moving average filters were applied iteratively by decreasing the resolution by 5 m, from 5 m to 41 m and from 51 m to 201 m in 10-m increments:

$$W(i,j) = 1, \quad \forall_i = -\left[\frac{S}{2}\right], \cdots, \left[\frac{S}{2}\right] \; \forall_j = -\left[\frac{T}{2}\right], \cdots, \left[\frac{T}{2}\right], \quad (2)$$

where S is the neighbourhood height, T is the neighbourhood width (represented by $\forall_i$ and $\forall_j$) and $W(i,j)$ is defined as the weight per specified filter (in this case = 1).

The low-pass moving filter smooths or removes high-frequency topographic variability from the 1-m resolution DEM as a function of the grid node centre and the neighbourhood cells (e.g. to 40 m, or 40 rows and columns). The neighbouring cells are then averaged using Equation 2 and the filter is then moved to the next grid node where the procedure is repeated (Pitas, 2000). After the range of low-pass filters mentioned above were tested, a 41 m × 41 m (including grid node centre) one was chosen because it is: (1) large enough to define residuals associated with small hummocks, hollows and isolated bogs within permafrost plateaus (problematic using high-filter resolutions); and (2) is not biased by dominant land cover types (problematic at lower filter resolutions). This filter most effectively and unambiguously classified the elevation gradient throughout the basin. Permafrost plateaus were then extracted by subtracting the 1-m resolution DEM from the detrended dataset and classified in ArcGIS.

A classification of the positive residuals (representing areas above the filtered mean, often plateaus), negative residuals (representing areas below the filtered mean, often bogs and channel fens) and vegetation height characteristics (canopy heights greater than 1.3 m) was used to determine the area and edges of the permafrost plateaus.

Canopy Shadow Modelling

The spatial distribution of within- and below-canopy shadows has varying influences on lateral permafrost degradation when combined with other driving mechanisms (e.g. soil moisture, soil texture, topographical characteristics, etc.). Canopy height and *f*cover models from LiDAR data were used to model spatial coverage of cumulative daily shadow fractions on the ground surface. The model used in this study is based on radiation models applied in ArcGIS and outlined in Rich (1990), Rich *et al.* (1999) and Fu and Rich (2000). These follow solar geometry models of Garnier and Ohmura (1970), Oke (1996) and others but extend beyond typical applications of the model by including LiDAR-derived estimates of *f*cover, elevation and the digital surface model (DSM) (canopy height, crown diameter and elevation). Numerous studies have applied radiation models to ellipsoidal primitives (stylised canopy shapes, for example, ellipsoids, cones, spheres, etc.) representing opaque tree canopy elements (e.g. Essery *et al.*, 2008; Ellis and Pomeroy, 2007), but few have applied such models to spatially measured canopy structural data and in areas of varying topography. A simple radiation model has been applied to LiDAR-measured tree canopies, assuming trees have transmissive characteristics based on leaf area. Here, we do not develop transmissive fractions (e.g. non-transmitting stems vs partly transmitting crowns). Primitive-based model studies (e.g. Ellis and Pomeroy, 2007) have examined transmissive fractions between stems and crowns, but applying this to LiDAR DSMs requires further study on the extraction of individual trees, stems and stem diameters (e.g. Reitberger *et al.*, 2007) and is beyond the scope of the current study. Here, it is assumed that the entire canopy is a transmissive medium.

According to forest mensuration plots on plateaus ($n = 23$), trees within the Scotty Creek sub-area are typically narrow (≤2-m radius crown), conical in shape, short (average heights <6 m) and have low foliage area (≤45%) that extends almost to the ground surface. LiDAR-measured trees within the CHM have been organised into individual shapes based on an IDW rasterisation procedure applied to the maximum z-height within a 1-m raster cell, and with a cell search radius of 2 m. A power of 2 has been applied within the IDW algorithm to create trees that are narrow and conical in shape. This, in combination with canopy *f*cover (used interchangeably with canopy transmissivity (e.g. Hardy *et al.*, 2004; Solberg *et al.*, 2006), but not including the effects of canopy clumping), is used to estimate canopy and ground surface shadowing. Canopy shadows were modelled for a single day during the thaw period (9 June), and another during the freezing period (11 November) per pixel location based on the upward-looking view factor (including topographic variability and tree canopy influences) and the amount of sky visible to the pixel location. For each pixel location, the maximum horizon angle and angle of incidence ($\widehat{\theta}$) are determined such that canopy or topography obstruction can be estimated from adjacent pixels using zenith (Z) and azimuth angles ($\widehat{\Omega}$), slope angle ($\widehat{\beta}$) and solar azimuth (Ω) (Oke, 1996):

$$\cos\widehat{\theta} = \cos\widehat{\beta}\cos Z + \sin\widehat{\beta}\sin Z\cos\left(\Omega - \widehat{\Omega}\right). \quad (3)$$

Shadow fractions from individual trees were determined based on the proportion of the sky visible to the pixel, so long as the sun was not blocked by the surrounding topography. The shape of shadow fractions were mapped based on individual tree height (h), vertical canopy cover or transmissivity (*f*cover) and crown radius (r_c) estimated using an IDW approach.

RESULTS

Reduction in Permafrost Area

Permafrost plateau area reduction from 2000 to 2008 was estimated at Scotty Creek using manually delineated vegetation cover as a proxy for permafrost plateau area (determined from IKONOS and digital aerial imagery) (Figure 2).

The total cumulative area of vegetated parts of permafrost plateaus as a percentage of the total was 49 per cent (± maximum of 12%) in 2000 but by 2008 this area had declined to 43 per cent (± maximum of 4%). Most of the change occurred at the edges of permafrost plateaus, illustrating that edges are prone to vegetation die-back as a result of thaw (Figure 2e). For the period 1947 to 2008, vegetated parts reduced by ~27 per cent (Figure 3) (Quinton *et al.*, 2010). These results are similar to those found in Beilman and Robinson (2003) who report that localised

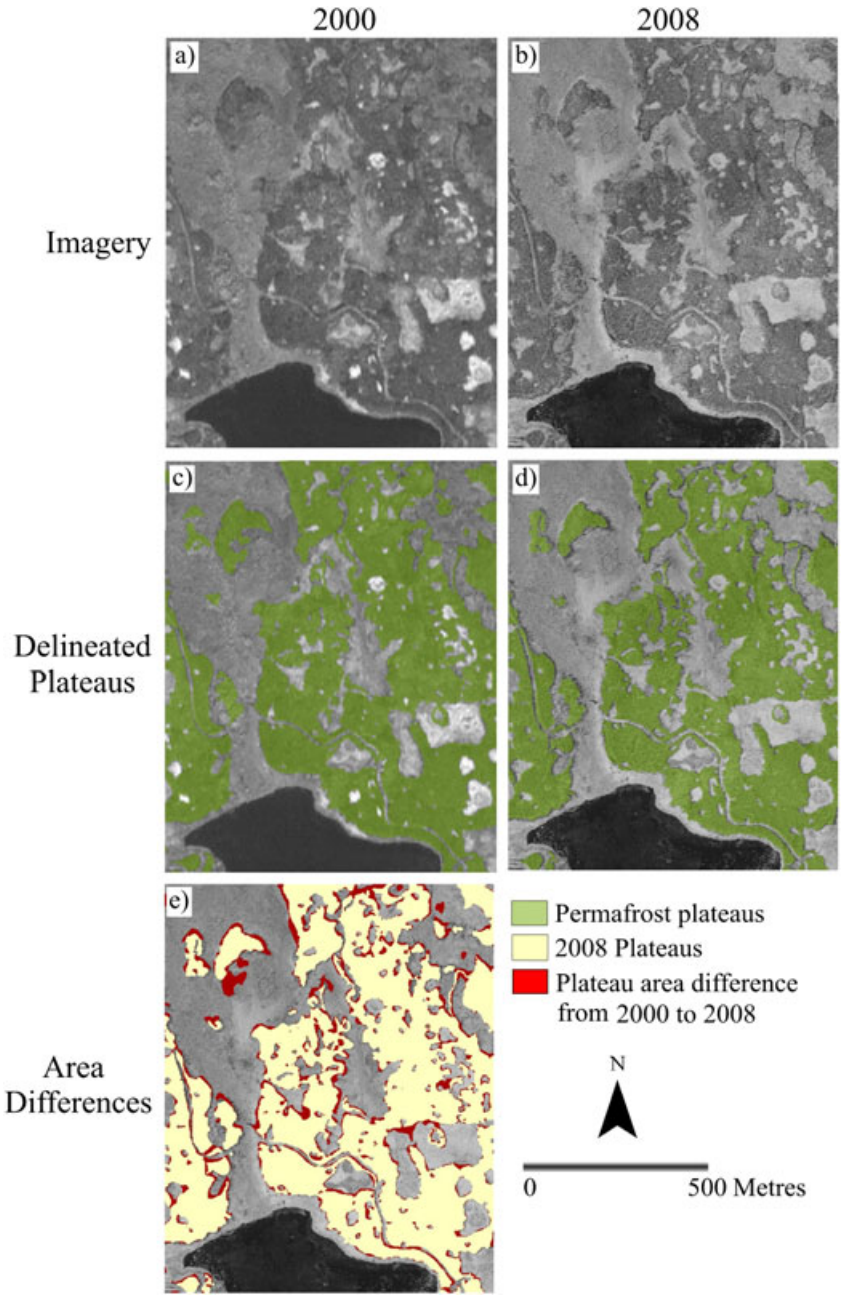

Figure 2 Scotty Creek from (a) IKONOS satellite imagery obtained in 2000 and (b) digital aerial photography obtained in 2008. Permafrost plateau areas were delineated (using vegetation cover as a proxy) in (c) 2000 and (d) 2008 and subtracted in (e) to illustrate plateau area change from 2000 to 2008. Grey areas in all images are fens, bogs and trails. This figure is available in colour online at wileyonlinelibrary.com/journal/ppp

permafrost degraded between 30 per cent and 65 per cent over 100 to 150 years as a result of increased mean annual air temperatures.

Decreasing plateau area found from 1947 to 2008 (Figure 3) resulted in the development of isolated bogs within plateaus, increasingly fragmented and small plateaus and increased length of plateau edges (after accounting for pixel resolution influences). Plateau edges in 1947 were approximately 22 000 m in length and increased linearly as a result of fragmentation to approximately 35 000 m in length in 2008 ($r^2 = 0.47$, $p = 0.2$) (Figure 4). However, if IKONOS data are not included (outlier caused by lower resolution pixels and an inability to resolve within-pixel edge complexity), the relationship improves ($r^2 = 0.99$). Perimeter-to-area ratios from 1947 to 2008 increased linearly from 0.03 to 0.08, illustrating that increased fragmentation within the landscape results in a greater percentage of plateau edges per unit area.

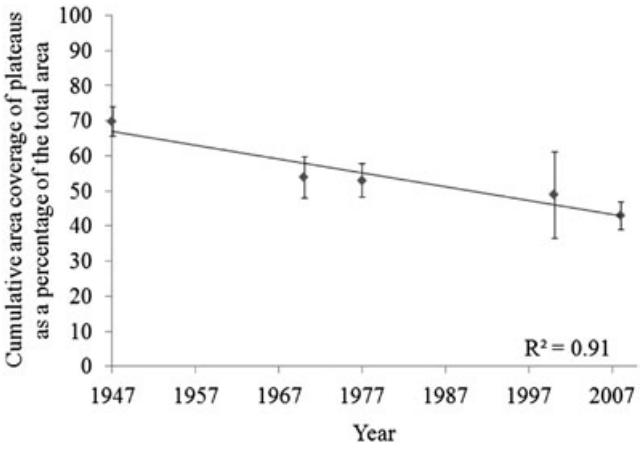

Figure 3 Cumulative permafrost plateau per cent area degradation (based on vegetation cover) at Scotty Creek determined from aerial photography (1947, 1970 and 1977), IKONOS imagery (2000) and digital imagery (2008). Error bars represent maximum and minimum per cent area extents when accounting for differences in pixel resolution, sun angles and geo-registration errors (described in Chasmer *et al.*, 2011).

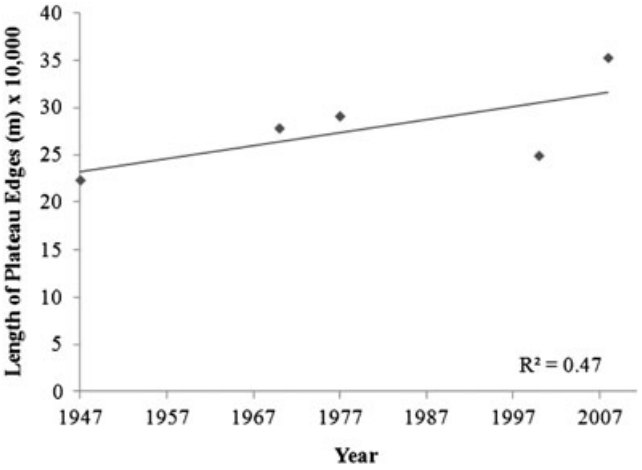

Figure 4 Length of classified plateau edges from 1947 to 2008 based on the datasets mentioned in Figure 3.

Spatial Variations of Vegetation Structure

The spatial variability of vegetation structure along the edges of permafrost plateaus may influence the radiation regime at the ground surface and may change spatial variability of permafrost thaw, especially as plateaus become increasingly fragmented. Vegetation structural differences at plateau edges, where change between 2000 and 2008 is most apparent (Figure 2e), may indicate a long-term trend of vegetation succession (Shur and Jorgenson, 2007). Trees and vegetation greater than 0.7 m in height cover approximately 57 per cent of the area of permafrost plateaus, not including gaps between trees (Figure 5). Yet only 10 per cent of bogs and fens contain vegetation with similar characteristics, and much of this vegetation is located within 15 m of permafrost plateau edges (Figure 6). Trees located at the edges of plateaus (Figure 2e) and in lower elevation areas within plateaus are shorter (average height ranging from 0.5 m to 1.7 m) and have less foliage (average canopy gaps comprise 80% to 95% of total tree cover) than trees located at higher elevations (average canopy height ranges from ~3 m to 6 m; area of canopy gaps = 40% to 60% of total tree cover) (Figure 5). This illustrates that canopy structural differences exist between vegetation found at plateau edges as opposed to vegetation located more centrally on higher elevation plateaus, especially where some trees at plateau edges have fallen. Fens and bogs have the greater proportions of short vegetation, with heights ranging from 0 m to 1 m and with low *f*cover of tall vegetation (0% to 2%).

Figure 6 shows the spatial distribution of vegetation heights in topographically detrended low-lying areas, along plateau edges and within plateaus. Plateau edges (Figure 6, yellow) with short vegetation located adjacent to bogs and

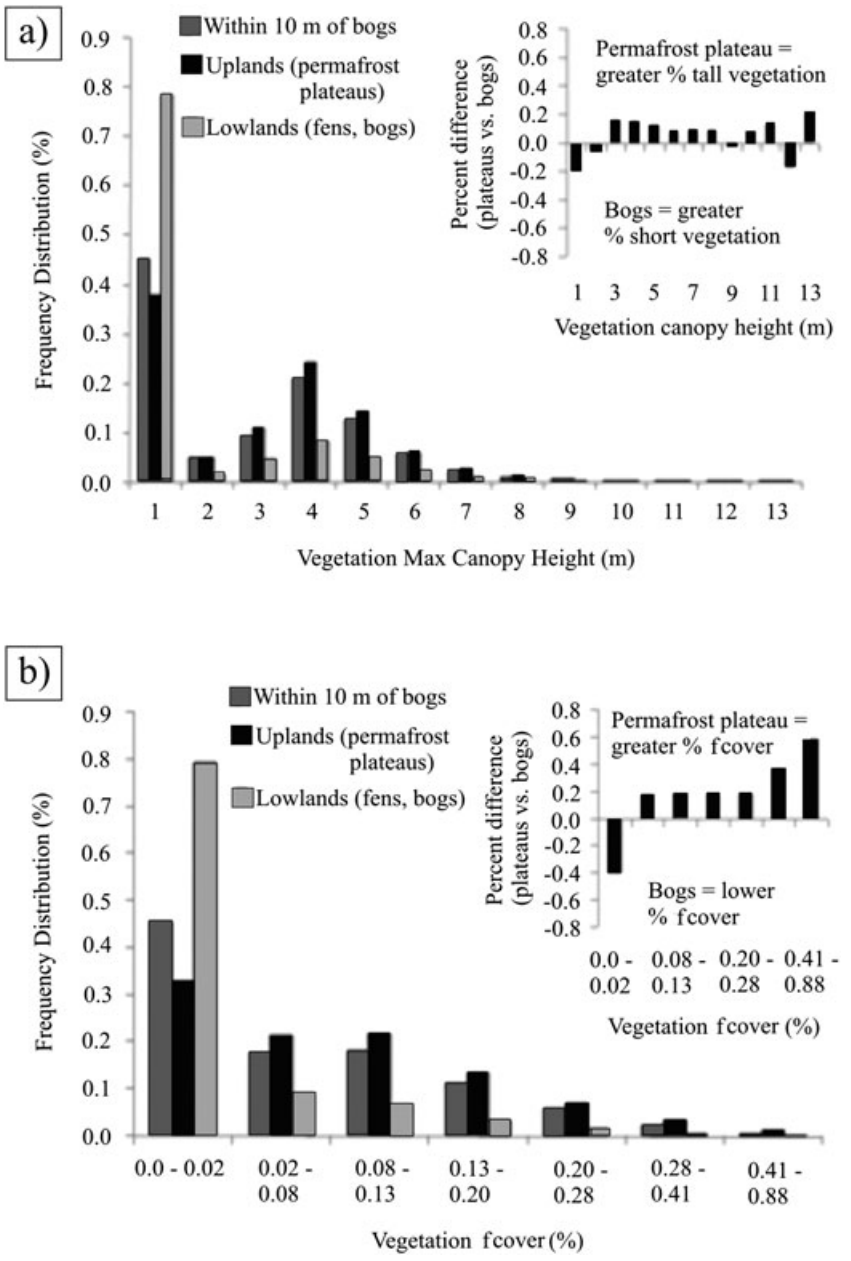

Figure 5 Frequency distributions of (a) maximum canopy height and (b) per cent canopy fractional cover (*f*cover) per land cover type. Per cent differences in canopy structure between permafrost plateaus and within the 10-m buffer areas surrounding bogs on plateaus are shown in the insets.

fens will likely undergo the most rapid changes in land cover. Slightly raised parts of the fen are prone to some vegetation growth, with canopies ranging in height from 1.5 m to 6 m. These areas may be indicative of vegetation succession and plateau development.

Spatial Variation of Insolation

Reduced biomass at the edges of permafrost plateaus (compared with that located at the centre of plateaus) can alter the radiation regimes at the ground surface, which may lead to increased rates of snow melt, ground heating and water runoff. This results in increased ground saturation, increased depth to permafrost and further vegetation die-back (Figures 2e and 3). Shur and Jorgenson (2007) suggest that vertical degradation of permafrost within subarctic regions may occur in areas where canopy cover does not protect permafrost from a warmer climate, such as by canopy shadowing. Figure 7 presents a simple conceptual model of permafrost thaw based on energy balance during the growing season.

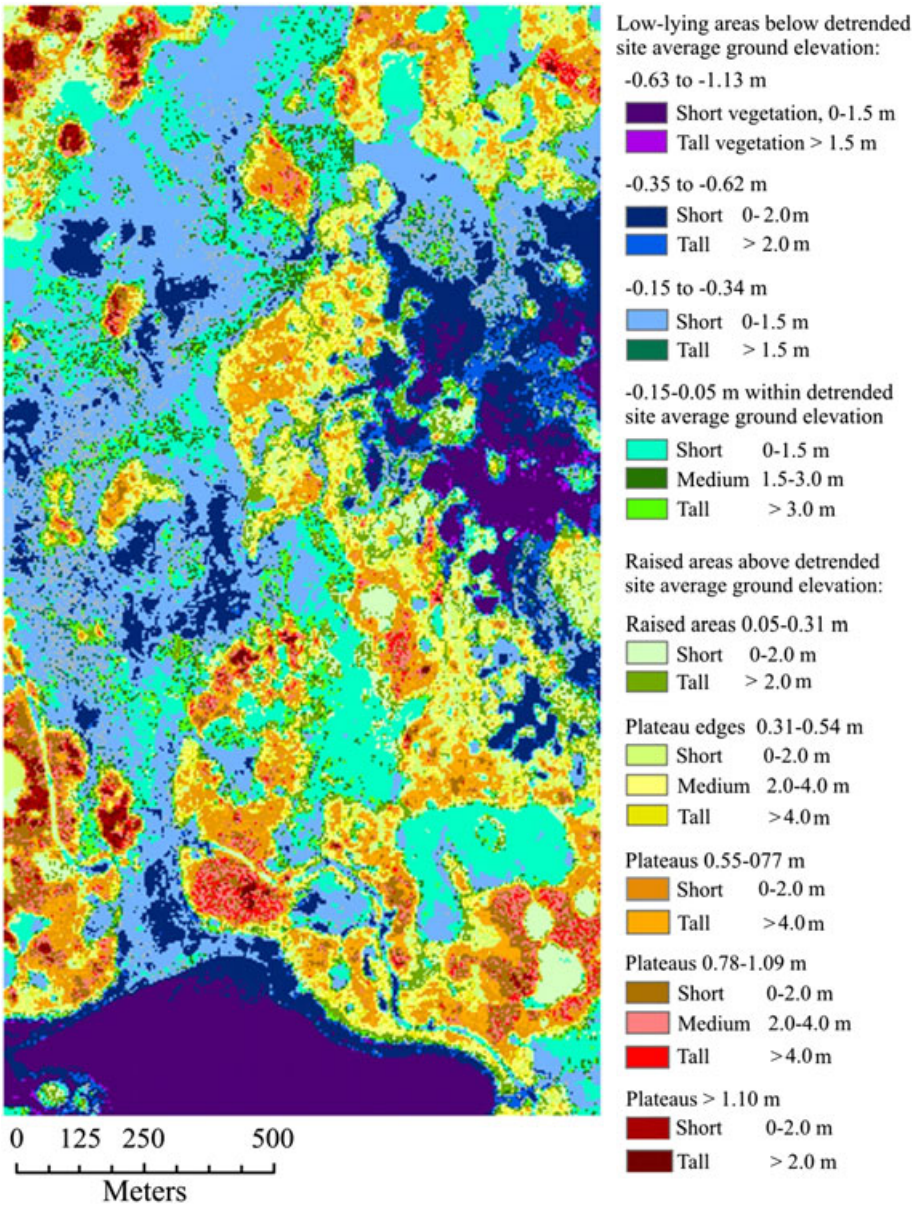

Figure 6 Land cover classification of low-lying areas and permafrost plateaus combined with vegetation canopy height characteristics. Cool colours represent low-lying areas, whereas warm colours represent plateaus and plateau edges.

To determine if differences in below-canopy radiation regimes occur within areas of varying canopy structural characteristics (PPclosed, PPopen and Bog), below-canopy radiation measurements were examined for 2007. Differences in the relative magnitudes of net shortwave radiation (K*) and net longwave radiation (L*) in relation to Q* were found at each site, especially in areas of closed vs open canopies (Figure 8). K* accounted for 92 per cent of Q* beneath the canopy at PPclosed and 81 per cent of Q* at PPopen and Bog (measured between 8 April and 17 August 2007 when data were available at all sites). Flux magnitudes also differed. Average daily below-canopy K* was greatest at the bog (244 Wm^{-2}) and least at PPclosed (143 Wm^{-2}). This resulted in a large per cent difference of K* at PPclosed when compared with that measured at the bog site (41%), and a smaller per cent difference in PPopen from bog (16%). Average daily L* was greatest at the bog (−57 Wm^{-2}), slightly less at PPopen (−50 Wm^{-2}) and least at PPclosed (−15 Wm^{-2}) (Figure 8). These results indicate that differences in canopy structural characteristics of permafrost plateaus, for example, an open vs a closed canopy, can significantly influence the below-canopy radiation regime, and especially longwave fluxes. In this case, the ground surface below an open-canopy forest located on a permafrost

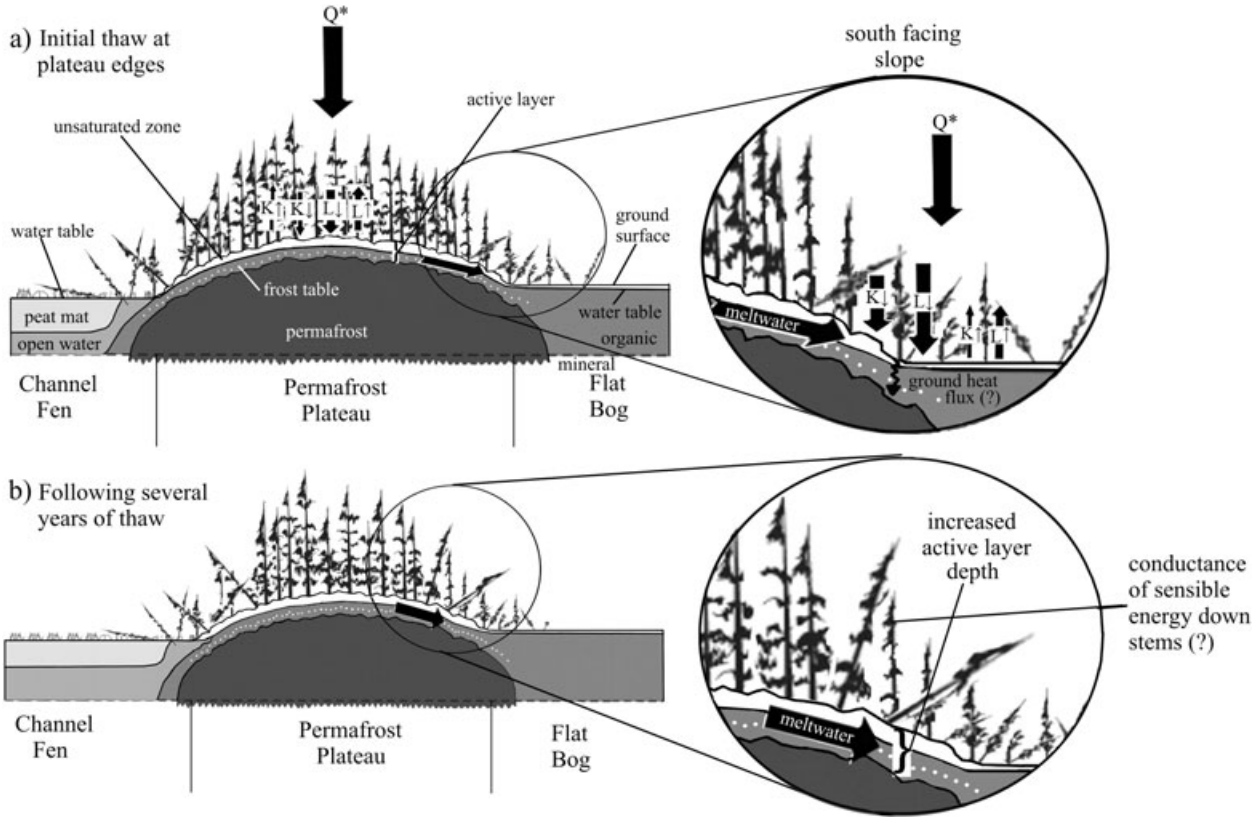

Figure 7 Schematic diagram of radiation influences on permafrost thaw during the growing season (modified from Quinton *et al.*, 2009). Magnitudes of energy and meltwater transfer are illustrated based on the width of arrows. (a) Warming of the ground surface (e.g. owing to warmer air temperatures) causes increased meltwater runoff, tree senescence and mortality at the edge of the plateau (see detail). (b) After several years of thaw, radiation incident on fallen and standing tree stems increases longwave fluxes and thaw of the active layer (see detail). Small hollows on plateaus aid in the movement of meltwater to bogs and the channel fen. Diagram does not include the influences of soil type/texture, plateau morphology (e.g. slope, aspect, size), or snow distribution. Question marks represent hypotheses not yet tested at this site.

plateau lost 74 per cent more energy to L* (on average) than a PPclosed. Increased amounts of below-canopy K* received by PPopen (30% greater than at PPclosed) and greater losses of L* indicate that more shortwave energy is received by the ground surface at PPopen.

Fluxes of K*, L* and Q* at open- and closed-canopy sites were strongly influenced by the relative magnitudes of incoming and outgoing short- and longwave radiation. K↓ and K↑ were greatest at the bog during the winter and summer periods (Figure 9), and similar below the canopy at PPopen and PPclosed. However, differences in L↓ were 10 per cent greater at the closed-canopy plateau site compared with that measured within an open canopy, and 14 per cent greater than L↓ measured at the bog site (Figure 9). Differences in L↓ between the open-canopy plateau and bog sites were much smaller (3%). These results illustrate the importance of canopies for absorption and re-emission of longwave fluxes from the canopy. Smaller differences in L↑ were found between open and closed canopies (0.9%), and between these sites and the bog (2% and 1% for closed and open canopies, respectively).

Modelling Radiative Flux based on Canopy Characteristics

To illustrate the spatial variability of canopy cover influences on below-canopy shadowing and incident K↓, cumulative shadow periods were modelled from canopy height and canopy *f*cover on 11 June and 9 November 2007 as examples of summer thaw and winter freeze periods. Figure 10a illustrates plateau area changes from 1977, 2000 and 2008, and Figure 10b shows areas that average at least one hour less of shadow in June and November. The daily (site) average cumulative shadow period was approximately 3.5 h in June (~20% of total 17-h daylight period) and 4 h in November (~57% of total 7-h daylight period). Areas with reduced periods of shadow such as at the edges of permafrost plateaus correspond well with permafrost area changes (Figure 10). From 1977 to 2008, 41 per cent of areas that had undergone reduced shadowing corresponded to plateau area reduction, while from 2000 to 2008, this increased to 54 per cent (excluding areas of sparse canopy cover within plateaus and within the fen (northwest corner))

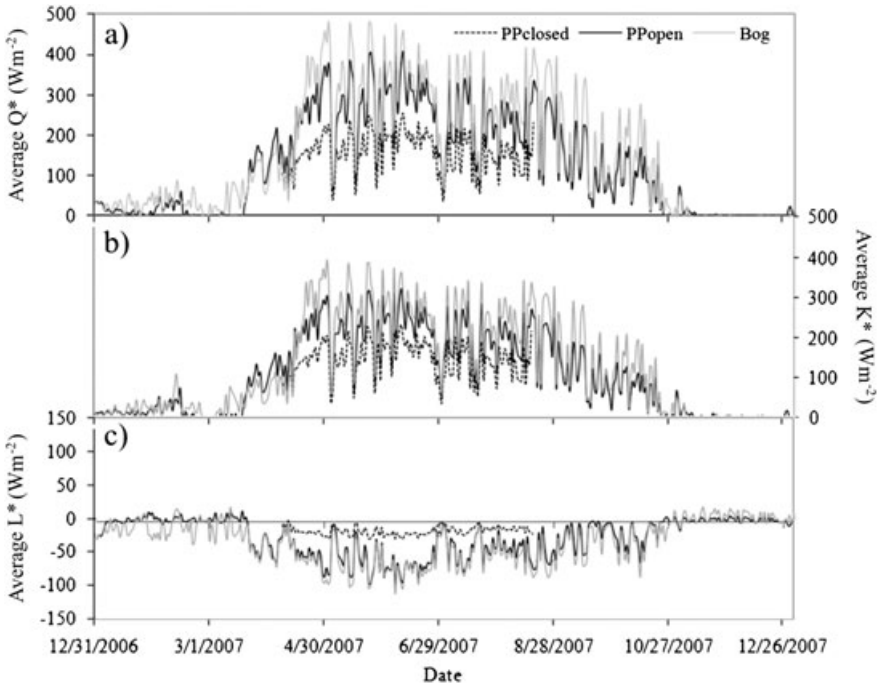

Figure 8 (a) Daily average net radiation (Q*), (b) daily average shortwave radiation (K*) and (c) daily average longwave radiation (L*) measured at an open-canopy permafrost plateau site (PPopen) and a bog site with no tree canopy (Bog) from 1 January to 31 December 2007 and at a closed-canopy permafrost plateau site (PPclosed) from 8 April to 17 August 2007.

(Figure 10b). Minor errors exist in the shadow area calculation for the latter because LiDAR reflections tend to underestimate measured canopy heights by ~9 per cent (e.g. Hopkinson *et al.*, 2005) since the laser pulses often are not able to reflect from the apices of narrow black spruce crowns. An 'artificial' increase in canopy height of 9 per cent (to compensate for underestimates) increases the area under shadow by 2.7 per cent of the total area in June and 3.4 per cent in November. This implies that correspondence between shadow area and plateau area reduction using the CHM is slightly over-estimated. Similarly, small errors exist for 1977 to 2008 (in this case, 1.8% in June and 2.4% in November). Plateau edges adjacent to bogs (southeastern part of the site), along linear features and trails, within small bogs located on plateaus and plateau areas adjacent to a large fen (central and southern parts of the site) were most strongly affected by reduced shadows. Approximately 67 per cent of the changed plateau area from 1977 to 2008 had southeast to westerly aspects when the DEM was resampled to 2 m (to remove small variations in topography). This indicates that large-area permafrost changes may relate to shortwave radiation, but complicating factors such as slope, soil type/conductivity and plateau shape/morphology are also likely important drivers of thaw. The relative importance of each is not yet known for Scotty Creek.

Anthropogenic and seismic disturbances, such as trails, cut lines and roads that remove protective vegetation, have resulted in reduced shadowing of the ground surface and lower ground surface elevations, depending on the age and width of the disturbance feature (Figure 10). Trails that are >10 m wide and older than 30 years of age (determined from historic aerial photography data and LiDAR) are 0.5 to 1.1 m lower in elevation than the surrounding permafrost plateau topography (within 2 m of the edge of the trail). Younger trails (less than 30 years of age) that are <5 m wide have ground surface elevations typically within 0.5 m of the plateau surfaces outside the trail (within 2 m). Quinton *et al.* (2009) note that linear features within the Scotty Creek basin have a combined length of 133.2 km, and likely have a strong influence on basin runoff when the width and age of these features are considered.

DISCUSSION AND CONCLUSIONS

A variety of different remote sensing and *in-situ* datasets were used to examine the influence of changing vegetation structure and radiation balance on large-area permafrost plateau degradation through time. The simple conceptual feedback model developed (Figure 7) is based on the idea that an increase in surface air temperature (e.g. through climate warming) could result in some permafrost thaw, which will increase the depth of the active layer. Increased meltwater runoff at plateau edges (Quinton *et al.*, 2009) and soil saturation cause loss of needles, tree mortality, and eventual uprooting or breaking of rotten tree boles, thereby reducing the shadowing properties of healthy tree canopies.

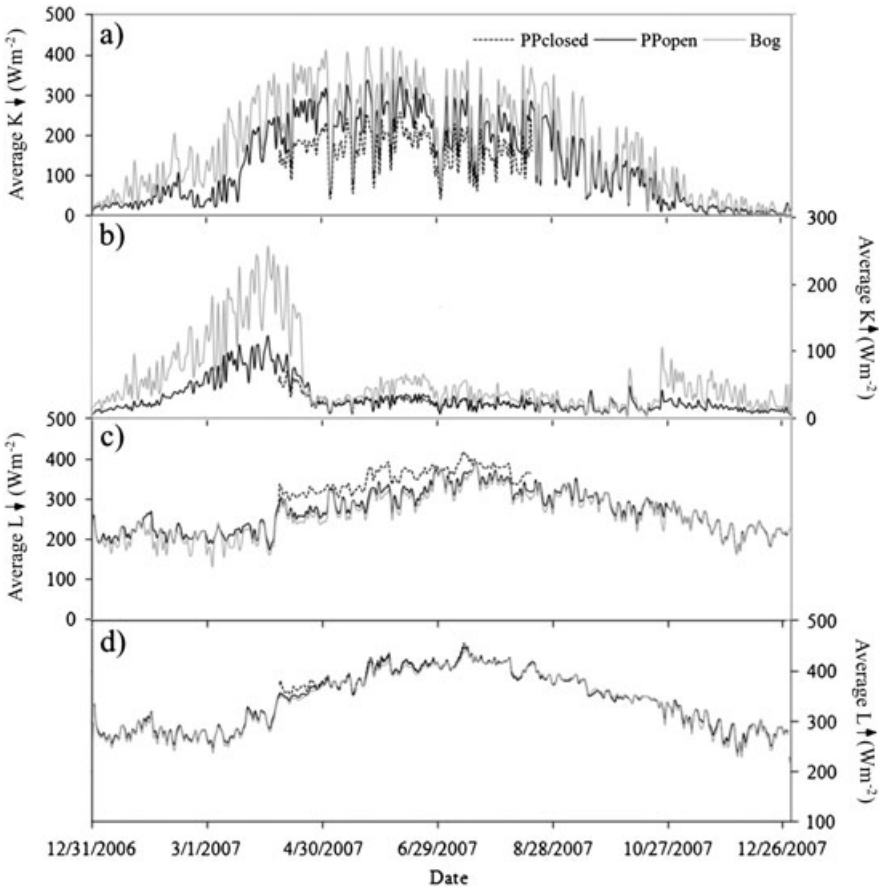

Figure 9 (a) Daily average incoming shortwave radiation (K↓), (b) daily average outgoing shortwave radiation (K↑), (c) daily average incoming longwave radiation (L↓) and (d) daily average outgoing longwave radiation (L↑) measured at an open-canopy permafrost plateau site (PPopen) and a bog site with no tree canopy (Bog) from 1 January to 31 December 2007 and at a closed-canopy permafrost plateau site (PPclosed) from 8 April to 17 August 2007.

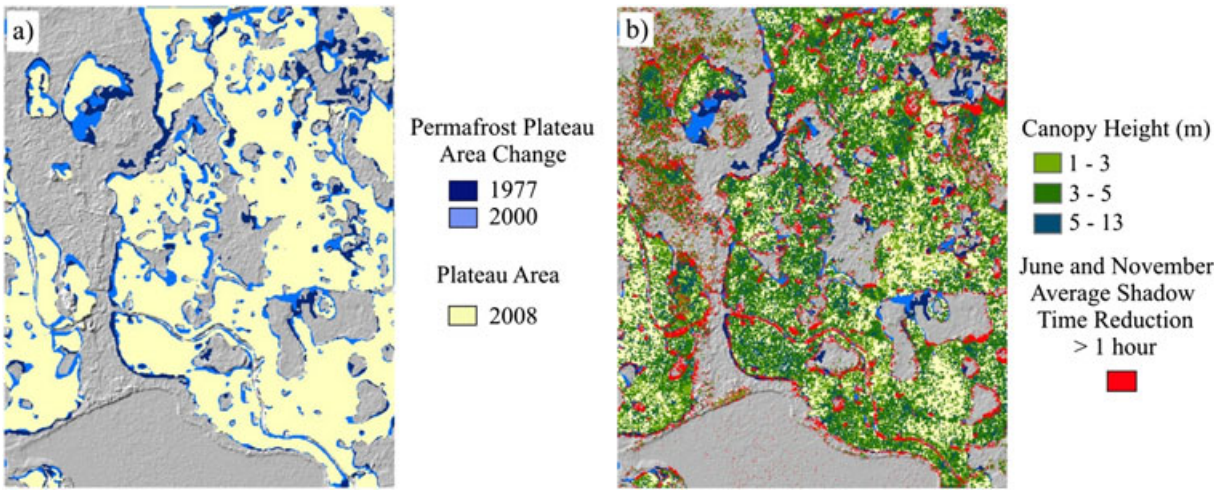

Figure 10 (a) Permafrost plateau area change for 1977 and 2000 compared to plateau area in 2008 (from aerial photography, IKONOS and digital imagery; (b) corresponding areas of reduced canopy shadowing at the edges of plateaus as a result of shorter canopies and lower biomass. Both (a) and (b) are overlaid onto a shaded relief digital elevation model.

Shortwave radiation incident on the ground surface at the edges of plateaus warms the soil profile and exacerbates permafrost thaw. Further, fallen (dead) tree boles intercepting incident shortwave radiation increase longwave fluxes within the canopy, and may transfer heat within the active layer (although this has not yet been tested). It is not known whether or not this positive feedback will continue indefinitely, as there also appear to be new stages of vegetation succession in the channel fen, which may be related to surface water routing. New vegetation growth may result in permafrost plateau development in the future.

Vegetation cover (as a proxy indicator of permafrost plateau area) decreased by ~27 per cent from 1947 to 2008 (Quinton *et al.*, 2010). Vegetation heights and canopy cover are greatest near the centre of plateaus, if they are not highly fragmented, but are reduced at plateau edges (Figure 5). Reduced tree heights at plateau edges are indicative of tree mortality (e.g. fallen/broken tree boles, reduced leaf area). Comparisons between radiation fluxes within structurally different canopy types showed that tree shadowing within closed canopies reduces shortwave fluxes incident on the ground surface and increases longwave fluxes within the upper canopy (Figures 8 and 9). As canopy cover is reduced, shortwave radiation incident on the ground surface increases causing ground heating (evidenced by slightly increased longwave fluxes from the soil surface) and the formation of depressions within the permafrost topography. For example, field measurements indicate that higher elevations are positively correlated to shallower depths of permafrost within five of seven transects (r^2 ranged from 0.47 to 0.76, $p < 0.01$, unpublished data). This confirms the results of Quinton *et al.* (2009), if we assume that the ground surface sinks (elevation decreases) as the depth to permafrost increases. This is also evident when examining the influence of linear features such as seismic exploration lines and roads on ground surface elevation. Once depressions have formed, water from surrounding areas drains into the depression causing an increase in the thickness of the thawed saturated layer, increased soil moisture and increased bulk thermal conductivity of the peat above the depression (Quinton *et al.*, 2009; Wright *et al.*, 2009).

At the basin scale, large areas of shadow reduction (calculated for June and November) at the edges of plateaus correspond with areas that have undergone biomass reduction from 1977 to 2008. Further, southeast to westerly facing slopes correspond with 67 per cent of the areas that have undergone change over the last 30 years, indicating that radiation is an important driver of permafrost change, along with other complicating factors that have not been examined in this study (e.g. plateau morphology, soil type/conductance, geology, etc., influences on soil moisture).

Lower resolution, historic remote sensing data therefore may be used to assess basin-scale variability, aided by airborne LiDAR, which can quantify plateau topographic and area change over a period of years (using baseline and subsequent surveys). Such technologies could be used to quantify major climatic influences on vegetation succession and permafrost plateau change, especially if climatic events strongly influence annual thaw penetration, as is suggested in Tarnocai *et al.* (2004). This corresponds with results of Quinton *et al.* (2009) who found a strong relationship between total water input and the depth to permafrost at the end of summer from 1999 to 2006. Greatest water input and deepening of the permafrost from 1999 to 2006 also corresponded with abnormally warm years (e.g. 2005–06).

ACKNOWLEDGEMENTS

We acknowledge support from the Improved Processes and Parameterisation for Prediction in Cold Regions network, including Dr Masaki Hayashi, Dr John Pomeroy, Liidlii Kue First Nation and Jean-Marie River First Nation. Dr Nicole Wright and Tyler Veness helped with instrumentation and fieldwork. LiDAR and digital imagery data were processed by Allyson Fox and Suzanne Monette at the AGRG. Funding for this project was provided by the Canadian Foundation for Climate and Atmospheric Sciences and the Natural Sciences and Engineering Research Council. Logistical support was provided by the Aurora Research Institute, Water Survey of Canada. We would also like to thank two anonymous reviewers, Dr Benjamin Crosby and Dr Antoni Lewkowicz for helpful comments and insights.

REFERENCES

Anisimov OA, Shiklomanov N, Nelson F. 2002. Variability of seasonal thaw depth in permafrost regions. A stochastic modeling approach. *Ecological Modelling* **153**: 217–227.

Beilman DW, Robinson SD. 2003. Peatland permafrost thaw and landform type along a climatic gradient. In *Proceedings of the Eighth International Conference on Permafrost*, Phillips M, Springman SM, Arenson LU (eds). A. A. Balkema: Lisse; 61–65.

Chasmer L, Hopkinson C, Treitz P, McCaughey H, Barr A, Black A. 2008. A lidar-based hierarchical approach for assessing MODIS fPAR. *Remote Sensing of Environment*. **112**: 4344–4357.

Chasmer L, Hopkinson C, Quinton W. 2011. Quantifying errors in discontinuous permafrost plateau change from optical data, Northwest Territories, Canada: 1947 to 2008. *Canadian Journal of Remote Sensing*. **36**(2): S211-S223.

Comiso JC and Parkinson CL. 2004. Satellite-Observed Changes in the Arctic. *Physics Today* Aug: 38–44.

Ellis C and Pomeroy J. 2007. Estimating subcanopy shortwave irradiance to melting snow on forested slopes. *Hydrological Processes* **21**: 2581–2593.

Essery R, Bunting P, Hardy J, Link T, Marks D, Melloh R, Pomeroy J, Rolands A, Rutter N. 2008. Radiative transfer modeling of a coniferous canopy characterized by airborne remote sensing. *Journal of Hydrometeorology. NASA Cold Land Processes Experiment (CLPX) Special Issue*. **9**: 228–241.

Fu P and Rich PM. 2000. A geometric solar radiation model and its applications in agriculture and forestry. In *Proceedings of the Second International Conference on Geospatial Information in Agriculture*

and Forestry, **I**: 357–364. Lake Buena Vista, 10–12 January 2000.

Garnier BJ and Ohmura A. 1970. The evaluation of surface variations in solar radiation income. *Solar Energy* **13**: 21–34.

Hardy JP, Melloh R, Koenig G, Marks D, Winstral A, Pomeroy JW, Link T. 2004. Solar radiation transmission through conifer canopies. *Agricultural and Forest Meteorology* **126**: 257–270.

Hayashi M, Goeller N, Quinton W, Wright N. 2007. A simple heat-conduction method for simulating the frost-table depth in hydrological models. *Hydrological Processes* **21**: 2610–2622.

Hopkinson C and Chasmer L. 2009. Testing a lidar intensity based model of canopy fractional cover across multiple forest ecozones. *Remote Sensing of Environment* **113**: 275–288.

Hopkinson C, Chasmer L, Sass G, Creed I, Sitar M, Kalbfleisch W, and Treitz P. 2005. Assessing vegetation height and canopy volume in a Boreal wetland complex using airborne scanning LiDAR. *Canadian Journal of Remote Sensing*. **31**(2): 191–206.

Morsdorf F, Kotz B, Meier E, Itten K, and Allgower B. 2006. Estimation of LAI and fractional cover from small footprint airborne laser scanning data based on gap fraction. *Remote Sensing of Environment*. **104**: 50–61.

National Wetlands Working Group. 1997. *The Canadian Wetland Classification System*, 2nd Edition. Warner BG, Rubec CDA, Wetland (eds.). Research Centre, University of Waterloo, Waterloo ON.

Oke TR. 1996. *Boundary Layer Climates*. Routledge: London; 435pp.

O'Sullivan D, Unwin DJ. 2003. *Geographic Information Analysis*. John Wiley & Sons: Hoboken, NJ.

Pitas I. 2000. *Digital Image Processing Algorithms and Applications*. John Wiley and Sons, New York; 419pp.

Pomeroy J, Rowlands A, Hardy J, Link T, Marks D, Essery R, Sicart J, Ellis C. 2008. Spatial variability of shortwave irradiance for snowmelt in forests. *Journal of Hydrometeorology CLPX Special Issue*. **9**: 1482–1490.

Quinton W, Hayashi M, and Chasmer L. 2009. Peatland hydrology of discontinuous permafrost in the Northwest Territories: Overview and synthesis. *Canadian Water Resources Journal*. **34**(4): 311–328.

Quinton W, Hayashi M, and Chasmer L. 2010. Permafrost thaw induced land-cover change in the Canadian subarctic: Implications for water resources. *Hydrological Processes Scientific Review*. In review.

Quinton WL, Hayashi M, and Pietroniro A. 2003. Connectivity and storage functions of channel fens and flat bogs in northern basins. *Hydrological Processes*. **17**: 3665–3684.

Reitberger J, Krzystek P, and Stilla U. 2007. Combined tree segmentation and stem detection using full waveform lidar data. In *Proceedings of the ISPRS Workshop on Laser Scanning 2007 and SilviLaser 2007*. Espoo, Finland.

Rich PM. 1990. Characterizing plant canopies with hemispherical photographs. *Remote Sensing Review*. **5**(1):13–29.

Rich PM, Wood J, Vieglais DA, Burek K, and Webb N. 1999. *Guide to HemiView: software for analysis of hemispherical photography*. Delta-T Devices, Ltd: Cambridge, England.

Robinson SD. 2002. Peatlands of the Mackenzie Valley: Permafrost, fire, and carbon accumulation. In *Proc. Carbon Dynamics of Forested Peatlands*, Edmonton, Alberta. 21–24.

Robinson SD, Moore, TR. 2000. The influence of permafrost and fire upon carbon accumulation in High Boreal peatlands, Northwest Territories, Canada. *Arctic, Antarctic, and Alpine Research*. **32**: 155–166.

Rouse WR. 1984. Microclimate of arctic tree line 2. Soil microclimate of tundra and forest. *Water Resources Research*, **20**(1): 67–73.

Rouse WR. 2000. Progress in hydrological research in the Mackenzie GEWEX study. *Hydrological Processes*. **14**: 1667–1685.

Shur YL and Jorgenson MT. 2007. Patterns of permafrost formation and degradation in relation to climate and ecosystems. *Permafrost and Periglacial Processes*. **18***:* 7–19.

Solberg S, Naesset E, Hanssen KH, and Christiansen E. 2006. Mapping defoliation during a severe insect attack on Scots pine using airborne laser scanning. *Remote Sensing of Environment*. **102**: 364–376.

Tarnocai C, Nixon FM, and Kutny L. 2004. Circumpolar-Active-Layer-Monitoring (CALM) sites in the Mackenzie Valley, northwestern Canada. *Permafrost and Periglacial Processes*. **15**: 141–153.

Todd KW, Csillag F, Atkinson PM. 2003 Three-dimensional mapping of light transmittance and foliage distribution using lidar. *Canadian Journal of Remote Sensing*. **29**(5): 544–555.

Wright N. 2009. Water and energy fluxes from a permafrost peat plateau: examining the controls on runoff generation. PhD thesis, Simon Fraser University, BC, Canada, 175pp.

Wright N, Hayashi M, Quinton WL. 2009. Spatial and temporal variations in active layer thawing and their implication on runoff generation in peat-covered permafrost terrain. *Water Resources Research* **45**: W05414. DOI: 10.1029/2008WR006880

